RSC Advances

ROYAL SOCIETY OF CHEMISTRY

www.rsc.org/advances

Journal Name

ARTICLE

Fabrication of Binary Components based Poly(ionic liquid) through "Grafting" and "Clicking" and their Synergistic Antifouling Activity

Received 00th January 20xx,
Accepted 00th January 20xx

DOI: 10.1039/x0xx00000x

www.rsc.org/

Wenwen Zhao,[a,b] Qian Ye,[a,*] Haiyuan Hu,[a] Xiaolong Wang,[a] and Feng Zhou[a,*]

Rational design of effective antifouling component is challenging but important for many fundamental and applied applications. Herein, we report the synergistic antifouling effects of nonionic, cationic and anionic compounds in combination with poly(ionic liquid) toward suppressing marine fouling. Firstly, nonionic, cationic and anionic compounds were respectively grafted onto substrate surfaces by light-induced click reaction of mPEG-SH, bromohexadecyl nicotinate (1-sulfydryl) ethyl ester and sodium 2-mercaptoethane sulfonate. Subsequently the poly(ionic liquid) brushes were grafted onto as-prepared surfaces via surface-initiated ring-opening metathesis polymerizations to obtain binary components modified surfaces. The antifouling properties of the sole component and binary components modified surfaces were evaluated by algae adhesion assay using *Navicula* spores. and *Dunaliella tertiolecta*. The antifouling results show that the binary compounds modified substrate surfaces exhibit better anti-adsorption performance than sole component, which is owing to the synergistic antifouling effect of binary components.

Introduction

Marine biofouling is a persistent worldwide problem that is detrimental to the maritime and aquatic industries,[1] the biofouling increases the hydrodynamic drag of ships, excessive consumption of fuel and initiation of corrosion, and cause serious problems and huge economic losses for marine industries and the navies.[2] Antifouling is the ability of specifically designed surface to remove or prevent the biofouling of wetted surfaces.[3] Infact, biofouling can occur wherever water is present, and poses significant risks to variety of structures, processes and applications. Therefore novel antifouling technologies, which could remove or inhibit the growth of biofouling products, are very important. Now, the introduction of toxic agents (such as arsenic, copper, tributyltin oxide and their organic derivatives) into marine coating have led to severe criticisms and resulted in the banning of TBT by the International Maritime Organization, because these biocides are extremely harmful to the marine environment.[2] This has stimulated considerable interest in the development of "Green" alternatives to biocide-based technologies to control fouling.[4]

Recently, polymer brushes are often used to alter surface properties due to their higher mechanical, chemical robustness, and higher long-term stability.[5] The polymer brushes with large exclusion volumes to inhibit protein and bacterial adhesion, or bactericidal functional groups, is of great importance in antifouling fields.[6] So polymeric materials were investigated extensively as environmentally benign anti-biofouling replacements.[7] Therefore, various types of polymers have been explored as anti-biofouling coatings including PEGylated polymers[2], hydrophobic polymers[8-9], hydrophilic polymers[10], amphiphilic polymer[11], zwitterionic polymer brushes[12], bioinspired polymers[13], which are suited for preparation of bio-inert interfaces to prevent protein adsorption, cell adhesion, and bacterial attachment. Poly(ethylene glycol) (PEG) and its derivatives acted as the commonly used antifouling materials and exhibit good antifouling attributed to the steric barrier, osmotic repulsion, excluded-volume effects, and the mobility or flexibility of the highly hydrophilic layer.[4,14,15] The polymer consisted of methoxy-terminated poly(ethylene glycol) (mPEG) conjugated to the L-3,4-dihydroxyphenylalanine (DOPA) exhibited a substantial decrease in attachment of both cells of *Navicula perminuta* and zoospores of *U. linza* as well as the highest detachment of attached cells under flow.[16] Recently, poly(ionic liquid)s (PILs) with consisting of ammonium, pyridinium, phosphonium, imidazolium etc. were found to play an important role in the fields of polymer chemistry and material science due to their particular properties, such as highly ion conductivity, inherent conductivity, high thermal stability, excellent mechanical properties and biocompatibility.[17,18] Attaching ionic liquid moieties to polymer chains is developing novel effective antimicrobial agents and anti-biofouling materials.[19,20] Tiller et al. have designed derivatizing poly(vinyl-N-hexylpyridinium bromide)-modified surfaces of the synthetic polymers high-density polyethylene, low-density polyethylene, polypropylene, nylon6/6, and poly(ethylene

terephthalate), which exhibited significant antibacterial properties against *S. aureus* and *E. coli* cells.[21] In our previous work, high-density poly(ionic liquid) brushes were grafted onto surfaces via surface-initiated ring-opening metathesis polymerizations (ROMP) and the as-prepared poly(ionic liquid) possess excellent anti-bacterial and anti-biofouling properties.[22]

Furthermore, cationic antimicrobials are also well-known for the development of self-sterilizing surfaces and widely used at hospital surfaces, surgical equipment, protective clothes in hospitals, food packaging materials, and everyday consumer products.[23] With respect to cationic antimicrobials quaternary ammonium salts (QAS) which can cause the death of cells by destroying the membrane integrity show great promise in the field of antimicrobial coatings.[24,25] Surfaces modified with QAS-containing polymers are effective for inhibiting microbial biofilm formation and killing a wide range of microorganisms.[26,27] Such as, pH responsive quaternary ammonium modified chitosan were prepared by Composto's group, which shows the weakest bacterial adhesion compared to silicon oxide surface and chitosan brush layer.[28] Anionic components that display a negative charge are another important functional antifouling agent such as 3-sulfopropyl methacrylate (SPMA), 4-styrenesulfonic acid sodium (NaSS) and glycidyl methacrylate (GMA), which displays excellent performance for preventing the adhesion of bacteria and microorganisms.[29] Terada et al. have reported that the biofilm formed on negatively charged surfaces were easily removed by liquid high shear washing.[30]

Although the various polymers possess antibiofouling characteristics, there remains a drawback using single component systems as many biofoulers release glycoprotein adhesives, Hence, the amphiphilic polymer with hydrophilic domains and hydrophobic domains have been demonstrated to be more effective antibiofouling properties than only a single polymeric component.[31,32] The surfaces modified with polymer brushes 2-hydroxyethyl methacrylate (HEMA) and (dimethylamino)ethyl methacrylate (DMAEMA) exhibited excellent resistance to bacterial fouling than single-component.[33] Herein, we present a novel strategy combining light induced-click reaction with surface-initiated ROMP to prepare binary components antifouling materials based on poly(ionic liquid). mPEG-SH, sodium 2-mercaptoethanesulfonate (MESNA) and bromohexadecyl nicotinate (1-sulfydryl) ethyl ester (SH-Py16) were grafted on surface respectively via light-induced click reaction, then graft poly(ionic liquid) brushes via surface-initiated ROMP, the synergistic antifouling properties of binary components antifouling materials based on poly(ionic liquid) have been evaluated. This work hopefully provides a promising component motif for the design of new effective antifouling surfaces.

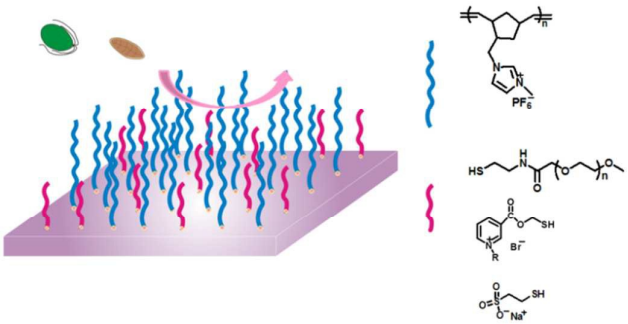

Scheme 1. Grafted binary components based on poly(ionic liquid) with antifouling properties

Experimental

2.1 Materials

Diphenyl(2,4,6-trimethylbenzoyl)phosphine oxide (TPO), nicotinoyl chloride hydrochloride (97%), 4-dimethylaminopyridine and sodium 2-mercaptoethanesulfonate (MESNA) were used as received from the Chemical Reagent Co. of J&K Chemical Ltd (Beijing, China). mPEG-SH was used as received from Shanghai Yare Biotech Co., Ltd. 2-hydroxy-1-ethanethiol and 1-Bromohexadecane were used as received from Chemical Reagent Company of Shanghai (Shanghai, China). Grubbs 2nd generation catalyst (benzylidene[1,3-bis(2,4,6-trimethylphenyl)-2-imidazolidinyl idene]-dichloro(tricyclohexylphosphine)ruthenium) were used as received from Sigma-Aldrich. The Anchor Agent N-(3,4-Dihydroxyphen-ethyl)bicyclo[2.2.1]hept-5-ene-2-carboxamide was synthesized according to the publication.[34] 1-norbornylmethylene-3-methylimidazolium hexafluoro phosphate(NM-MIm-PF_6) was synthesized according to the previous report.[22] Dichloromethane (China) was purified by distillation over CaH_2.

2.2 Synthesis of Bromohexadecyl nicotinate (1-sulfydryl) ethyl ester (SH-Py16)

Nicotinoyl chloride hydrochloride (1.78 g, 10 mmol) was first placed into a 50 ml round-bottomed flask with 15 ml dichloromethane, followed by adding 4-dimethylaminopyridine (1.22 g, 10 mmol) and 2-hydroxy-1-ethanethiol (0.78 g, 10 mmol) at room temperature. After 24 h, the solution was then purified by extraction with water and the residual solvent was evaporated under reduced pressure to give a viscous liquid. Then the product (0.18 g, 1 mmol) and 1-Bromohexadecane (0.31 g, 1 mmol) were placed into a 25 mL round-bottomed flask with acetonitrile (10 ml). The reaction mixture was stirred for 24 h at 80 °C under Ar. After cooling, the solution was then precipitated by excessive petroleum ether. The precipitate was washed with petroleum ether, yielding the final product SH-Py16.

^{1}H-NMR (400 MHz, $CDCl_3$) δ 9.95 (d, J = 6.0 Hz, 1H, H-1), 9.71 (s, 1H, H-5), 8.99 (d, J = 8.0 Hz, 1H, H-3), 8.34 (m, 1H, H-2), 5.17 (t, J = 7.2 Hz, 2H, H-10), 4.56 (t, J = 6.4 Hz, 2H, H-7), 3.26 (s, 1H, H-9), 2.97 (s, 2H, H-8), 2.06 (s, 2H, H-11), 1.22-1.39 (m, 26H, H-(12-24)),0.87 (t, J = 7.2 Hz, 3H, H-25)

^{13}C-NMR (100 MHz, $CDCl_3$) 160.9 (C-6), 149.0 (C-1), 145.5 (C-3), 145.2 (C-5), 130.3 (C-4), 128.8 (C-2), 68.4 (C-10), 62.8 (C-7), 32.0 (C-23), 31.9 (C-11), 29.7-29.0 (C13-22), 26.1 (C-12), 23.1(C-8), 22.7 (C-24), 14.1(C-25),

HRMS (ESI+): for $C_{24}H_{42}NO_2S$ M^+: calculated: 408.2931, found: 408.2887.

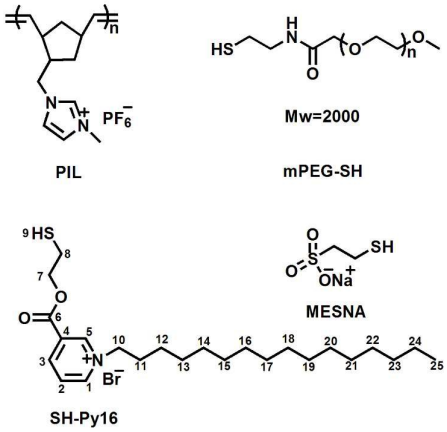

Scheme 2. Structure of the poly(1-norbornylmethylene-3-methylimidazolium hexafluorophosphate) (PIL), mPEG-SH, bromohexadecyl nicotinate (1-sulfydryl) ethyl ester (SH-Py16) and sodium 2-mercaptoethanesulfonate (MESNA).

2.3 Preparation of mPEG modified titanium surfaces

The preparation and modification of TiO_2 nanowires were described in our previous work[22]. In a quartz tube, the initiator modified TiO_2 nanowires (50 mg) and mPEG-SH (80 mg, 0.04 mmol), and TPO (2.8 mg, 0.008mmol) were added in 5 mL dichloromethane and irradiated at 365 nm UV lamp at room temperature under Ar flow for 30min. They were then carefully rinsed (three times) with pure dichloromethane and then dried under vacuum at 45 °C for 12 hours. MESNA-TiO_2 nanowires and Py16-TiO_2 nanowires have been prepared by the similar method.

2.4 Preparation of binary components based poly(ionic liquid)s modified titanium surfaces

The mPEG-TiO_2 nanowires were immersed in a solution of Grubbs 2nd generation catalyst (10 mg) in 5 mL dichloromethane and then placed in a flask under Ar flow for 20 min. They were then carefully rinsed (three times) with pure dichloromethane in order to remove the excess catalyst. The [Ru]-functionalized samples were immersed in 5 mL of freshly prepared solutions of NM-MIm-PF_6 (IL) (0.25 M) in dichloromethane. These polymerizations were carried out at room temperature under Ar protection for 2 hours. MESNA-PIL and Py16-PIL modified Ti surfaces were prepared in the same way.

2.5 Characterization

Navicula sp. and *Dunaliella tertiolecta* were obtained from Freshwater Algae Culture Collection at the Institute of Hydrobiology, Chinese Academy of Sciences and cultured respectively in Erdschreiber medium and Dunaliella medium at room temperature for attachment experiments. Three replicates of the samples were evaluated for settlement of *Navicula* and *Dunaliella* spores. A uniform Ti sample was included in the assay and served as a control for direct comparison. Just before the experiment, all the samples were filled with deionized water and were transferred to medium for 1 h without exposure to air. The *Navicula* and *Dunaliella* spores inoculum was adjusted to 10^6 Spores mL^{-1}. The spores settled on the different substrates surfaces were grown for 24h in an illuminated incubator at room temperature. After 24h growth, the substrates were rinsed three times. Cells counted were obtained from ten random fields of view on each of 3 replicate samples.

^{1}H-NMR and ^{13}C-NMR spectra were recorded on a 400 MHz spectrometer (Bruker AM-400) using $CDCl_3$ as solvent. Chemical composition information of samples were obtained by X-ray photoelectron spectroscopy (XPS); the measurement was carried out on a PHI-5702 multi-functional spectrometer using Al Ka radiation (29.35 eV) and the binding energies were referenced to the C 1s line at 284.8 eV from adventitious carbon. FT-IR spectra were recorded on a TENSOR 27 instrument (BRUCKER). The morphologies were investigated by transmission electron microscopy (TEM) (Hitachi Model JEM-2010). Atomic force microscopy (AFM) measurements were performed on an Agilent Technologies 5500 AFM using a MacMode Pico SPM magnetically driven dynamic force microscope. Zeta potential was measured using a Nano-ZS 90 Nanosizer (Zetasizer Nano ZS, Malvern Instruments Ltd., UK).Scanning electron microscopy (SEM) images were carried out on a field-emission scanning electron microscopy (JSM-6701F, JEOL Inc., Japan). Optical micrographs were taken on OLYMPUS BX51.

Results and discussion

Rational design of antifouling surfaces is challenging, but it is important for many fundamental and applied applications. Herein, binary components-modified surfaces were prepared through light-induced click reactions and SI-ROMP (Scheme 3).

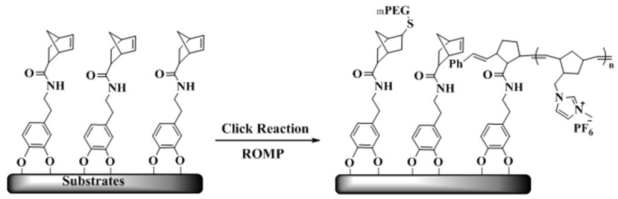

Scheme 3. Grafting PEG and poly(ionic liquid) binary antifouling components on substrates.

Prior to the antifouling investigation, binary components successful modification were ascertained by XPS, IR and TEM. XPS measurements were used to monitor the surface chemical composition change of each reaction step. Fig. 1A displays the XPS full survey spectra of bare TiO_2 nanowires, initiator-modified TiO_2 nanowires, mPEG-TiO_2 nanowires and mPEG-PIL-TiO_2 nanowires. Successful anchoring of initiator onto TiO_2 nanowires was ascertained by XPS.[22] After 0.5h click reaction, the C 1s high-resolution spectrum of mPEG-TiO_2

nanowires shows the peak components at binding energies of about 286.4 eV and 284.8 eV attributed to the C-O bonds and the C-C bonds in Fig. 1B. As shown in Fig. 1C, the N 1s peak of initiator-TiO_2, mPEG-TiO_2 nanowires display one peak with a binding energy at 398.3 eV. After 2 h SI-ROMP of the monomer NM-MIm-PF_6, poly(ionic liquid) brushes grafting was confirmed by a sharp increase of N signal at 400.6 eV attributable to ammonium nitrogen (N^+), and the presence of strong F 1s (686.4 eV) and P 2p (136.5 eV) signals. In Fig. S2B and S2E, MESNA and SH-Py16 modified TiO_2 nanowires were confirmed by the appearance of Na and Br signals at 1071.6 and 62.5 eV, respectively. The N1s spectrum of Py16-TiO_2 nanowires shows the broad peak at binding energies of about 399.8 eV and 401.8 eV attributed to the O=C–N bonds in the catecholic initiator and ammonium nitrogen (N^+) in Fig. S3. As shown in Fig. S2C and F, MESNA-PIL-TiO_2 and Py16-PIL-TiO_2 nanowires also display a sharp increase of N signal attributable to ammonium nitrogen (N^+) at 401.8 eV and F 1s at 686.4 eV after 2 h SI-ROMP of NM-MIm-PF_6.

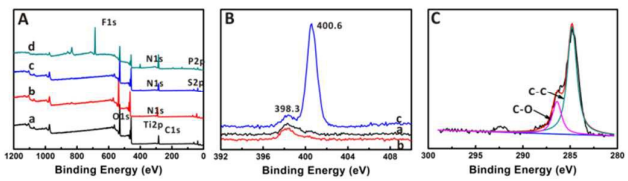

Fig. 1 (A) XPS survey spectra of (a) TiO_2 nanowires, (b) initiator-modified TiO_2 nanowires, (c) mPEG-TiO_2 nanowires and (d) mPEG-PIL-TiO_2 nanowires. (B) N 1s spectra of (a) initiator- TiO_2 nanowires, (b) mPEG-TiO_2 nanowires and (c) mPEG-PIL-TiO_2 nanowires. (C) The high-resolution spectrum of the C 1s region of mPEG-TiO_2 nanowires.

The successful grafting of mPEG-SH and PIL on TiO_2 nanowires was also confirmed by FT-IR spectroscopy (Fig. 2). Blank TiO_2 shows a featureless spectrum except for the wide absorption peaks of absorbed water above 3000 cm^{-1}.[22] Fig. 2 demonstrates the FT-IR spectrum evolution from blank TiO_2 nanowires, initiator modified TiO_2 nanowires, mPEG-TiO_2 nanowires, to mPEG-PIL-TiO_2 nanowires (2 h). FT-IR analysis of the mPEG-modified surfaces (Fig. 2-c) reveals characteristic adsorption bands at 1238, 1398 and 1650 cm^{-1}, which can be attributed to C-O stretching vibration, C-H vibration mode and C=O stretching vibration of the alkyl chains, which indicate the attachment of mPEG-SH onto TiO_2 nanowires. After click reaction with MESNA, the S=O stretching bands of the sulfonate group have been observed in the region of 1183 to 1293 cm^{-1} and the symmetric S=O stretching mode appears near 1156 cm^{-1} in Fig. S4-a.[35] As shown in Fig. S4-c, after the modification of Py16-SH, the characteristic adsorption bands at 1130 and 1301 cm^{-1} appeared, which can be attributed to C=O stretching vibration, and the adsorption bands at 2855 and 2924 cm^{-1} are owed to C-H stretching vibration mode of the alkyl chains. After grafting the second component PIL, the strong absorption peak at 841 cm^{-1} is attributed to the absorbance of P-F stretching modes of PF_6^-, and the characteristic vibration bands at 1571, 1460 and 1159 cm^{-1} correspond to the imidazolium ring cation,[22] indicating that PIL has been successfully grafted onto TiO_2 nanowires.

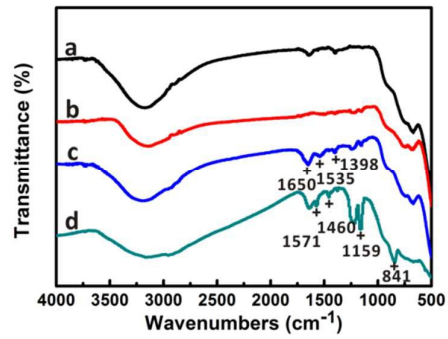

Fig. 2 FT-IR spectra of (a) TiO_2 nanowires, (b) initiator-modified TiO_2 nanowires, (c) mPEG-TiO_2 nanowires and (d) mPEG-PIL-TiO_2 nanowires.

The zeta potentials (ζ) of TiO_2 nanowires before and after modification with mPEG, mPEG-PIL were investigated by a Nano-ZS 90 Nanosizer in ethanol media. The zeta potential of bare TiO_2 nanowires is -5.71 ± 0.9 mV, after modification with mPEG, the zeta potential becomes positive (-1.2± 0.3 mV). Then, after grafting the poly(ionic liquid) brushes on mPEG-TiO_2 nanowires, the zeta potential becomes more positive (31.9 ± 3.4 mV) due to imidazolium cation (Table S1.). The zeta potentials of MESNA-TiO_2 nanowires and Py16-TiO_2 nanowires are -29.9 ± 0.4 and 22.0 ± 1.2 mV, respectively, after grafting PIL, the zeta potentials of MESNA-PIL nanowires and Py16-PIL nanowires also became more positively, 21.5 ± 1.8 and 31.1 ± 3.4 mV, respectively.

The presence of mPEG-SH and PIL layer was directly observed by TEM characterization. Fig. 3 shows transmission electron microscopic (TEM) images of the surface morphology of mPEG-SH and mPEG-PIL coated TiO_2 nanowires. From Fig. 3A, the TiO_2 nanowires surfaces were coated with a very uniform mPEG-SH coating layer and the interface boundary is very clear, the thickness of mPEG-SH is near to 3 nm. After modification with PIL (Fig. 3B), the thickness of polymer layer increased to 15 nm, which has a lighter color than the bulk TiO_2 nanowires grafting PIL. From the above results, we can conclude that the TiO_2 nanowires had been successfully modified with mPEG-SH and PIL.

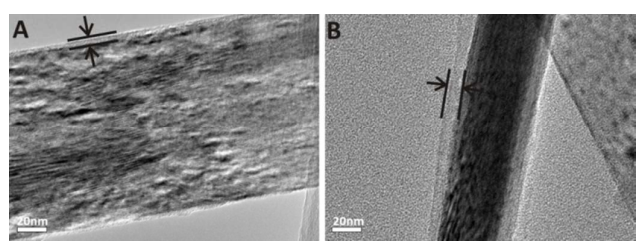

Fig. 3 TEM images of (A) mPEG-modified TiO_2 nanowires and (B) mPEG-PIL-modified TiO_2 nanowires.

To further support the results, atomic force microscopy (AFM) was used to investigate the surface morphology of

mPEG-SH and mPEG-PIL modified Ti surfaces. Fig. 4 shows 3μm × 3μm tapping-mode AFM phase images of Ti, mPEG-Ti and mPEG-PIL-Ti. Before modification (Fig. 4A), small particles are uniformly distributed over the whole Ti surface. After modification with mPEG-SH onto the Ti surface (Fig. 4B), the roughness of the mPEG-Ti surface becomes low (RMS decreased from 0.874 nm to 0.505 nm), which shows that mPEG-SH have masked onto Ti surface. The roughness of MESNA-Ti and Py16-Ti also decrease (RMS decreases to 0.606 nm and 0.693 nm respectively, Fig. S5). After modification with the second component PIL, small grains, uniformly distributed over the whole surface, and the rms roughness of mPEG-PIL-Ti increases to 0.720 nm (Fig. 4C). After 2h ROMP of of the monomer NM-MIm-PF_6, the roughness of MESNA-PIL and Py16-PIL modified Ti surfaces have the same varying trend (RMS increases to 0.91 nm and 0.791 nm respectively, Fig. S5), indicating that PIL has been successfully grafted onto Ti surfaces.

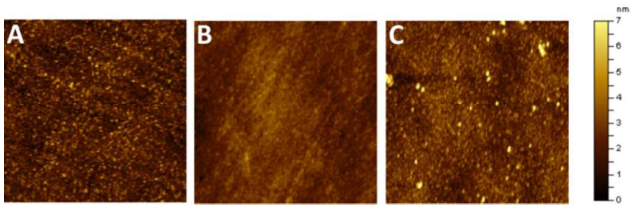

Fig. 4 3μm × 3μm AFM images for surfaces (A) bare Ti, (B) mPEG-Ti, (C) mPEG-PIL-Ti.

Fouling results from the settlement and growth of marine organisms on the surfaces of submerged object. The first stage of biofouling involves the formation of biofilms which provides the condition of microfouling. However, marine organisms may settle at the same time, such as zoospores of the alga *Ulva linza* and cyprids of the barnacle *Amphibalanus amphitrite* (*A. amphitrite*)[34]. Therefore, preventing the settlement of microalgae is the important objective for an effective antifouling coating.

In order to investigate the anti-biofouling effect of different components, mPEG-Ti, mPEG-PIL-Ti, MESNA-Ti, MESNA-PIL-Ti, Py16-Ti and Py16-PIL-Ti were prepared and the modified substrates were thereafter tested in biological assays with two ubiquitous biofouling organisms: organic *Navicula* and *Dunaliella* spores under artificial seawater conditions for 24 h. The results of the settlement assays of *Navicula*. sp and *Dunaliella tertiolecta* on different surfaces are shown in Fig. 5, and we could observe significant differences in settlement behavior of *Navicula*. sp and *Dunaliella tertiolecta*. As shown in Fig. 5A, the average spores density of mPEG-SH, MESNA and SH-Py16 modified surfaces were 1088 ± 49, 1248 ± 91, 1160 ± 145 spores mm^{-2}, after 24 h in the *Navicula* spores culture media. Meanwhile, a similar trend was observed for the settlement of *Dunaliella* on as-prepared surfaces (Fig. 5B). The average *Dunaliella* spores density of mPEG-SH, MESNA and SH-Py16 modified surfaces were 2573 ± 243, 2802 ± 145, 2601 ± 141 spores mm^{-2}, respectively.

It was observed that mPEG-SH modified surfaces exhibited a lower settlement than that of the MESNA and SH-Py16 modified surfaces, which could be attributed to the highly hydrated PEG chains in water[14]. In comparison to the uncoated Ti surface, the fractions of settlement on the anionic MESNA-Ti surface exhibited the lowest resistance to microalgae, with a decrease in *Navicula* and *Dunaliella* adhesion of 13.3% and 8.6%, which might be due to electrostatic interaction between anionic surface and the positively charged lysine of microalgae.[8] As seen in Fig. 5A-f and 5B-f, the Py16-Ti surface exhibited a higher efficiency in deterring microalgae than the MESNA-Ti surface, with settlement fractions of 19.4% and 15.2%, respectively. In Fig. 5A, after introducing the second antifouling component PIL, mPEG-SH, MESNA and SH-Py16 with PIL resulted in a reduction of approximately 38%, 4.2% and 46.3% for *Navicula* adhesion, respectively. As in the case of *Dunaliella* in Fig. 5B, the dramatic reduction in the settlement on mPEG-SH and SH-Py16 modified surfaces was observed, 47.7% and 49.5%, respectively. So, the PIL can enhance the antifouling performance of mPEG-SH and SH-Py16 based surface. The MESNA-PIL-Ti shows poor inhibition effect for spore, because the electronegativity of MESNA has decreased the catalytic activity of Grubbs catalyst.[36] The results indicate that the binary compounds based poly((ionic liquid) grafting surfaces exhibited better anti-adsorption performance than sole component owing to the synergistic effect.

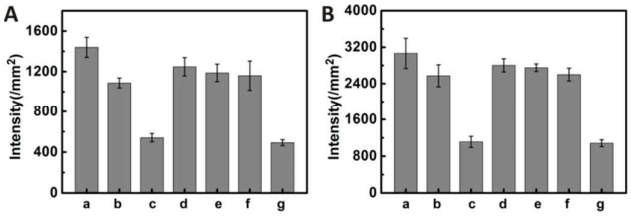

Fig. 5 Organic (A) *Navicula* and (B) *Dunaliella* spores settlement data on (a) bare Ti, (b) mPEG-Ti, (c) mPEG-PIL-Ti, (d) MESNA-Ti, (e) MESNA-PIL-Ti, (f) Py16-Ti, (g) Py16-PIL-Ti.

The settled *Navicula* and *Dunaliella* spores on different surfaces were fixed in 2.5% glutaraldehyde in phosphate buffer pH 7.4 for 3h and processed in the conventional way for SEM (dehydration, criticalpoint drying and sputter-coating with gold) before viewing. The adhesive form of *Navicula* and *Dunaliella* spores on different surfaces was not identical. Fig. 6 and 7 show the conformation of *Dunaliella* and *Navicula* spores on bare Ti, mPEG-Ti, mPEG-PIL-Ti, MESNA-Ti, MESNA-PIL-Ti, Py16-Ti, Py16-PIL-Ti surfaces respectively. Spores can adhere to the surfaces via a secreted adhesive glycoprotein.[37] In Fig. 6, it is clear that there is a circular blot around *Dunaliella* spore. After modification with PIL, the circular blot became small. Fig. 7 shows the adhesion of *Navicula* spores on different surfaces. After immersion in the culture suspension for 3h, it can be seen that there is a blot around the spore in Fig. 7A, B, D and F. Meanwhile, there is few blot around the spore adhesion on surfaces after grafting PIL. This phenomenon proves that binary components are very effective against

microalgae.

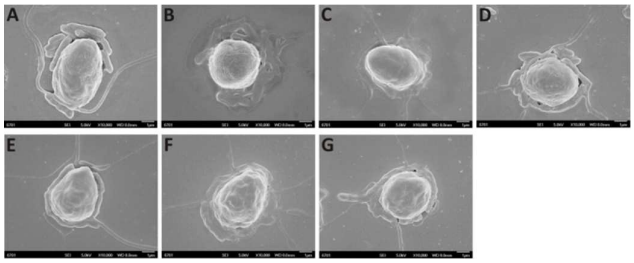

Fig. 6 SEM images of *Dunaliella tertiolecta* settlement on (A) bare Ti, (B) mPEG-Ti, (C) mPEG-PIL-Ti, (D) MESNA-Ti, (E) MESNA-PIL-Ti, (F) Py16-Ti, (G) Py16-PIL-Ti.

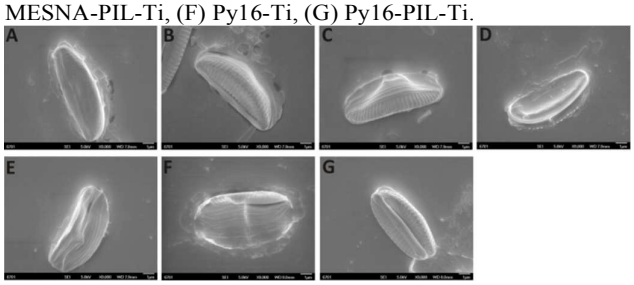

Fig. 7 SEM images of *Navicula* spores settlement on (A) bare Ti, (B) mPEG-Ti, (C) mPEG-PIL-Ti, (D) MESNA-Ti, (E) MESNA-PIL-Ti, (F) Py16-Ti, (G) Py16-PIL-Ti.

Conclusions

Binary components based on poly(ionic liquid) were successfully grafted onto surfaces via a novel methods that combine light-induced click reaction with surface-initiated ring-opening metathesis polymerizations. We have prepared three types of binary components consisting of nonionic, cationic and anionic compounds in combination with poly(ionic liquid) from catecholic initiator, and their antifouling abilities were evaluated by microalgae assays. The experiment result showed that the nonionic, cationic and anionic compounds modified surfaces own anti-biofouling effect and show different degrees of resistance to *Navicula* and *Dunaliella* spores settlement. After grafting the second component poly(ionic liquid), the binary components modified titanium surfaces exhibited better anti-adsorption performance than single component, which is attributed to the synergistic effect of anti-fouling compounds and poly(ionic liquid). The results indicate that the binary components antifouling materials can prevent biofouling effectively, and provide a novel method for design of effective anti-biofouling materials.

Acknowledgements

This work was financially support by NSFC (21434009, 21204095, 51203173) and Key Research Program of CAS (KJZD-EW-M01).

Notes and references

a. State Key Laboratory of Solid Lubrication, Lanzhou Institute of Chemical Physics, Chinese Academy of Sciences, Lanzhou 730000, China.
b. University of Chinese Academy of Sciences, Beijing 100049, China.
Fax: +86-931-4968163; Tel: +86-931-4968466;
E-mail: yeqian213@gmail.com and zhouf@licp.cas.cn

1 M. R. Detty, R. Ciriminna, F. V. Bright and M. Pagliaro, *Acc. Chem. Res.*, 2014, **47**, 678-687.
2 D. M. Yebra, S. Kiil and K. Dam-Johansen, *Prog. Org. Coat.*, 2004, **50**, 75-104.
3 F. Hong, L. Xie, C. He, J. Liu, G. Zhang and C. Wu, *J. Mater. Chem. B*, 2013, **1**, 2048-2055.
4 J. A. Callow and M. E. Callow, *Nat. Commun.*, 2011, **2**, 244-253.
5 X. Lin, Q. He and J. Li, *Chem. Soc. Rev.*, 2012, 41, 3584-3593.
6 Ye, Q and Zhou, F Antifouling Surfaces Based on Polymer Brushes. In Antifouling Surfaces and Materials, Zhou, F., Ed. Springer, New York, 2015, pp. 55-81.
7 J. F. Schumacher, M. L. Carman, T. G. Estes, A. W. Feinberg, L. H. Wilson, M. E. Callow, J. A. Callow, J. A. Finlay and A. B. Brennan, *Biofouling*, 2007, **23**, 55-62.
8 W. J. Yang, K. G. Neoh, E. T. Kang, S. S. Lee, S. L. Teo and D. Rittschof, *Biofouling*, 2012, **28**, 895-912.
9 X. Ding, S. Zhou, G. Gu and L. M. Wu, *J. Mater. Chem.*, 2011, 21, 6161-6164.
10 H. Chen, M. Zhang, J. Yang, C. Zhao, R. Hu, Q. Chen, Y. Chang and J. Zheng, *Langmuir*, 2014, **30**, 10398-10409.
11 W. J. Yang, K. G. Neoh, E. T. Kang, S. L. M. Teo and D. Rittschof, *Prog. Polym. Sci.*, 2014, 39, 1017-1042..
12 W. W. Zhao, Q. Ye, H. Y. Hu, X. L. Wang and F. Zhou, *J. Mater. Chem.* B, 2014, 2, 5352-5357.
13 Gu, Y. J and Zhou, S. X, Functional Polymer Coatings: Principles, methods, and applications. In Novel Marine Antifouling Coatings: Antifouling Principles and Fabrication Methods, Wu, L. M. and Baghdachi, J., Ed. Wiley-VCH, Weinheim, 2015, pp. 296-337.
14 I. Banerjee, R. C. Pangule and R. S. Kane, *Adv. Mater.*, 2011, **23**, 690-718.
15 J. Y. Ryu, I. T. Song, K. H. Lau, P. B. Messersmith, T. Y. Yoon and H. Lee, *ACS Appl. Mater. Interfaces*, 2014, **6**, 3553-3558.
16 A. Statz, J. Finlay, J. Dalsin, M. Callow, J. A. Callow and P. B. Messersmith, *Biofouling*, 2006, **22**, 391-399.
17 F. Zhou, Y. Liang and W. Liu, *Chem. Soc. Rev.*, 2009, **38**, 2590-2599.
18 J. P. Hallett and T. Welton, *Chem. Rev.*, 2011, **111**, 3508-3576.
19 S. K. Sharma, G. S. Chauhan, R. Gupta and J. H. Ahn, *J Mater. Sci-Mater. M.*, 2010, **21**, 717-724.
20 J. Pernak, K. Sobaszkiewicz and I. Mirska, *Green Chem.,* 2003, **5**, 52-56.
21 J. C. Tiller, S. B. Lee, K. Lewis and A. M. Klibanov, *Biotechnol. Bioeng.*, 2002, **79**, 465-471.
22 Q. Ye, T. T. Gao, F. Wan, B. Yu, X. W. Pei, F. Zhou and Q. J. Xue, *J. Mater. Chem.,* 2012, **22**, 13123-13131.
23 J. Hoque, P. Akkapeddi, V. Yadav, G. B. Manjunath, D. S. Uppu, M. M. Konai, V. Yarlagadda, K. Sanyal and J. Haldar, *ACS Appl. Mater. Interfaces*, 2015, **7**, 1804-1815.
24 B. Gottenbos, H. C. van der Mei, F. Klatter, P. Nieuwenhuis and H. J. Busscher, *Biomaterials*, 2002, **23**, 1417-1423.
25 J. Hazzizalaskar, N. Nurdin, G. Helary and G. Sauvet, *J. Appl. Polym. Sci.*, 1993, **50**, 651-662.
26 S. Ye, P. Majumdar, B. Chisholm, S. Stafslien and Z. Chen, *Langmuir*, 2010, **26**, 16455-16462.
27 A. Contreras-Garcia, E. Bucio, G. Brackman, T. Coenye, A. Concheiro and C. Alvarez-Lorenzo, *Biofouling*, 2011, **27**, 123-135.
28 H. S. Lee, M. Q. Yee, Y. Y. Eckmann, N. J. Hickok, D. M. Eckmann and R. J. Composto, *J. Mater. Chem.*, 2012, **22**, 19605-19616.
29 M. Krishnamoorthy, S. Hakobyan, M. Ramstedt and J. E. Gautrot, *Chem. Rev.*, 2014, **114**, 10976-11026.
30 A. Terada, K. Okuyama, M. Nishikawa, S. Tsuneda and M. Hosomi, *Biotechnol. Bioeng.*, 2012, **109**, 1745-1754.

31 S. Krishnan, N. Wang, C. K. Ober, J. A. Finlay, M. E. Callow, J. A. Callow, A. Hexemer, K. E. Sohn, E. J. Kramer and D. A. Fischer, *Biomacromolecules*, 2006, **7**, 1449-1462.

32 K. A. Pollack, P. M. Imbesi, J. E. Raymond and K. L. Wooley, *ACS Appl. Mater. Interfaces,* 2014, **6**, 19265-19274.

33 Y. Sui, X. L. Gao, Z. N. Wang and C. J. Gao, *J. Membr. Sci.*, 2012, **394**, 107-119.

34 Q. Ye, X. L. Wang, S. B. Li and F. Zhou, *Macromolecules*, 2010, **43**, 5554-5560.

35 N. M. Correa, P. A. R. Pires, J. J. Silber and O. A. El Seoud, *J Phys Chem B*, 2005, **109**, 21209-21219.

36 C. Samojłowicz, M. Bieniek and K. Grela, *Chem. Rev.* 2009, **109,** 3708-3742.

37 J. A. Callow, M. P. Osborne, M. E. Callow, F. Baker and A. M. Donald, *Colloid Surf. B*, 2003, **27**, 315-321.

Graphic for abstract

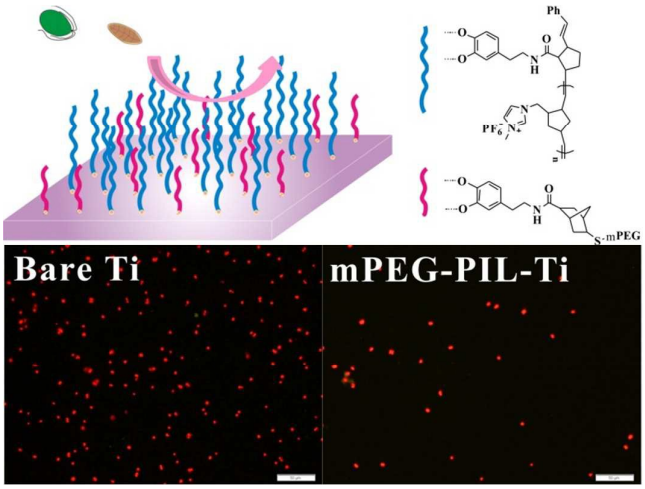

Grafting binary components mPEG-poly(ionic liquid) via “grafting from” and “clicking” reaction for antifouling applications.